

# The effect of strain on the electronic properties of MoS<sub>2</sub> monolayers

Soon-Dong Park<sup>1a</sup> and Sung Youb Kim<sup>\*2</sup>

<sup>1</sup>*School of Materials Science and Engineering, Ulsan National Institute of Science and Technology, 50 UNIST-gil, Ulsu-gun, Ulsan 689-798, Republic of Korea*

<sup>2</sup>*Department of Mechanical Engineering, Ulsan National Institute of Science and Technology, 50 UNIST-gil, Ulsu-gun, Ulsan 689-798, Republic of Korea*

*(Received April 3, 2015, Revised October 22, 2015, Accepted November 4, 2015)*

**Abstract.** We utilize first-principles calculations within density-functional theory to investigate the possibility of strain engineering in the tuning of the band structure of two-dimensional MoS<sub>2</sub>. We find that the band structure of MoS<sub>2</sub> monolayers transits from direct to indirect when mechanical strain is applied. In addition, we discuss the change in the band gap energy and the critical strains for the direct-to-indirect transition under various strains such as uniaxial, biaxial, and pure shear. Biaxial strain causes a larger change, and the pure shear strain causes a small change in the electronic band structure of the MoS<sub>2</sub> monolayer. We observe that the change in the interaction between molecular orbitals due to the mechanical strain alters the band gap type and energy.

**Keywords:** molybdenum disulfide; density functional theory; mechanical strain; band gap engineering

## 1. Introduction

Following the discovery of graphene, a large number of experimental and theoretical works (Novoselov and Geim 2004, Novoselov and Geim 2005, Zhang and Tan 2005, Lee and Wei 2008, Dan and Lu 2009, Kim and Park 2010) have reported on the two-dimensional nanomaterials and their outstanding properties. Graphene, one of the most extensively studied two-dimensional materials, exhibits distinctive physical properties such as 1 TPa of stiffness, ultrahigh electronic transport, chemical stability, and ability to sense nanoscale quantities. In addition to graphene, MoS<sub>2</sub>, NbSe<sub>2</sub>, and BN have been mentioned as next-generation two-dimensional nanomaterials. The optical spectroscopy measurement of a MoS<sub>2</sub> monolayer by Mak and Lee (2010) demonstrated that the MoS<sub>2</sub> monolayer exhibited a direct band-gap of 1.9 eV. Recently, Radisavljevic and Radenovic (2011) reported that the mobility of the MoS<sub>2</sub> monolayer using hafnium oxide (HfO<sub>2</sub>) for a metal-oxide-semiconductor field-effect Transistor (MOSFET) was increased to 200 cm<sup>2</sup>/Vs, indicating the possibility of using a MoS<sub>2</sub> monolayer as a MOSFET channel.

---

\*Corresponding author, Professor, E-mail: [sykim@unist.ac.kr](mailto:sykim@unist.ac.kr)

<sup>a</sup>Ph.D. Student, E-mail: [simao@unist.ac.kr](mailto:simao@unist.ac.kr)

The previous studies (Mak and Lee 2010, Radisavljevic and Radenovic 2011) show that a single layer of MoS<sub>2</sub> is very attractive for a range of applications, such as semiconductor or optoelectronic devices. For semiconductor applications, and especially for use as MOSFET channels, the mobility of the carriers becomes the most important factor. In conventional semiconductor materials, the mobility of the electron increases as the band-gap energy decreases, and similar trends have been shown for carbon nanotubes (CNTs) and graphene nanoribbons (GNRs) by Obradovic and Kotlyar (2006). To utilize a MoS<sub>2</sub> monolayer as a MOSFET channel, we have to find an effective way to reduce the band-gap energy of the MoS<sub>2</sub> monolayer, because 1.9 eV is too high compared to other conventional semiconductor materials. In addition, for the application of optoelectronic devices, it is imperative to keep the band-gap of the MoS<sub>2</sub> monolayer direct for the purpose of photon excitation.

In this paper, we utilize first-principles calculations with density-functional theory to investigate whether mechanical strain is able to control the band-gap energy and band-gap type of a MoS<sub>2</sub> monolayer. Toward this end, we apply uniaxial, biaxial, and pure shear strains to a single layer of MoS<sub>2</sub>, and discuss the effect of mechanical strain on the variation in the band-gap energy and the direct-to-indirect band gap transition.

## 2. Computational method

Our calculations were performed using the density functional theory method (DFT) implemented in the Vienna *ab-initio* simulation package (VASP) by Kress and Hafner (1993), Kress *et al.* (1996a, b). The exchange and correlation energy functional was adopted with the local density approximation (LDA) by Perdew and Zunger (1981) and the generalized gradient approximation (GGA) of Perdew-Wang 91 by Perdew and Chevary (1992). The interactions between the core and valence electrons were described by the ultra-soft (US) pseudo-potential

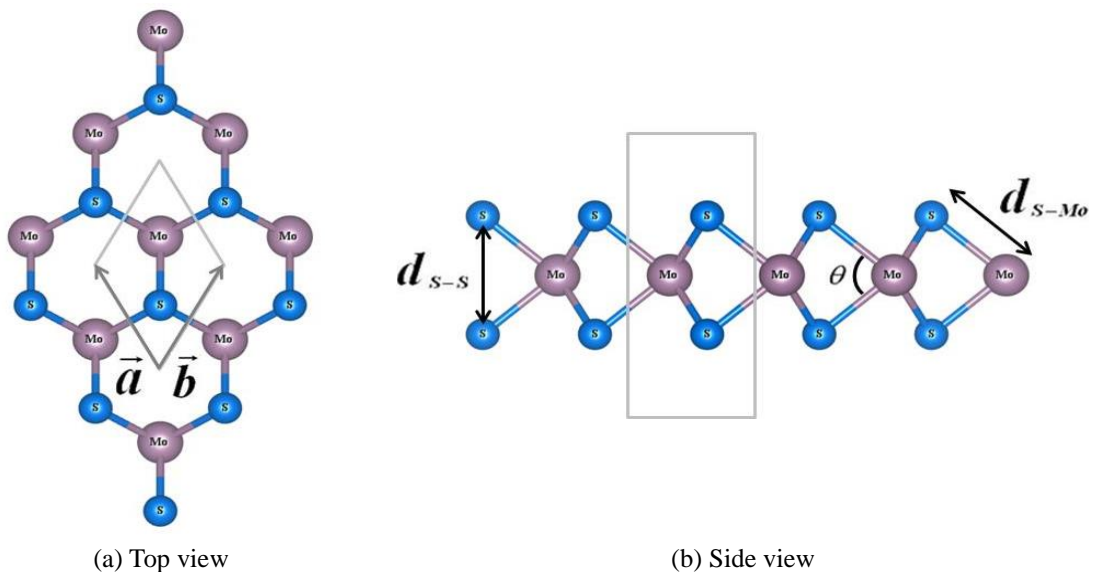


Fig. 1 The MoS<sub>2</sub> monolayer unit cell

Table 1 The calculated structural parameters and properties of a MoS<sub>2</sub> monolayer: Lattice constant  $a$ , bond lengths  $d_{S-Mo}$  and  $d_{S-S}$ , bond angle  $\theta_{S-Mo-S}$ , cohesive energy per MoS<sub>2</sub> unit cell

	$a$	$d_{S-Mo}$	$d_{S-S}$	$\theta_{S-Mo-S}$	$E_c$ (eV)	$E_g$ (eV)
GGA	3.19	2.42	3.13	80.65	15.76	1.64
LDA	3.13	2.38	3.11	81.47	18.96	1.82
Reference*	3.20	2.42	3.13	80.69	15.55	1.58
	3.11	2.37	3.11	81.62	19.05	1.87
Reference**	3.20					1.90

\*Reference: Ataca and Ciraci (2011)

\*\*Reference: Mak and Lee (2010), Joensen and Crozier (1987)

(Vanderbit 1990) for the LDA and by the projector augmented wave (PAW) pseudo-potential (Bloch 1994) for the GGA, respectively. The electrons of wavefunctions were extended up to a cutoff energy of 400 eV in a plane-wave basis set. To simulate the two-dimensional properties, the vacuum separation along the out-of-plane direction is set to more than 10 Å. All calculations were relaxed until forces on each ion become less than 0.01 eV/Å. The 5×5×1 Monkhorst-Pack (Monkhorst and Pack 1976) meshes were used for sampling the Brillouin zone. The unit cell for the MoS<sub>2</sub> monolayer adopted the 1×1 structure shown in Fig. 1, including one molybdenum atom and two sulfur atoms. Before applying strain to the MoS<sub>2</sub>, we calculated the structural parameters, cohesive energy, and band gap energy, and summarized them along with other reported values (Mak and Lee 2010, Ataca and Ciraci 2011, Joensen and Crozier 1987) in Table 1. The LDA result is in good agreement with the experimental value of the band-gap energy, and therefore the later calculations were conducted based on the LDA.

### 3. Results

The electronic band structure of a single layer of unstrained MoS<sub>2</sub> and some interesting wave functions at the  $\Gamma$  and K points are shown in Fig. 2. As shown in Fig. 2(a), we found that the valence band maximum (VBM) and the conduction band minimum (CBM) are located at the same reciprocal space point, K point, which indicates that the band-gap type of the MoS<sub>2</sub> monolayer is direct, in contrast to its bulk counterpart. (Mak and Lee 2010) The band-gap energy is found to be 1.9 eV at the K point, which is 0.6 eV higher than the band-gap energy of bulk MoS<sub>2</sub>. (Kam and Parkinson 1982) This direct band-gap and higher band-gap energy of the MoS<sub>2</sub> monolayer, unlike its bulk counterpart, exhibit the unique electronic characteristics of two-dimensional nanomaterials, and thus show the potential for various applications in electronic and photonic devices.

We plot the wave functions of electron orbitals of an unstrained MoS<sub>2</sub> monolayer at the  $\Gamma$  point and K point in Figs. 2(b) to (e), so that we can analyze the variation in the electronic band-gap of a MoS<sub>2</sub> monolayer under mechanical strain, the results of which we present later in this paper. At the K point, the CBM and the VBM are anti-bonding states of a  $d$ -orbital of molybdenum and a  $p$ -orbital of sulfur atoms, as shown in Figs. 2(b) and (c), respectively. In addition, the VBM and the second highest valence band at the  $\Gamma$  point show mainly the non-bonding state of a  $d$ -orbital of molybdenum (d) and the bonding state of a  $d$ -orbital of molybdenum and a  $p$ -orbital of sulfur

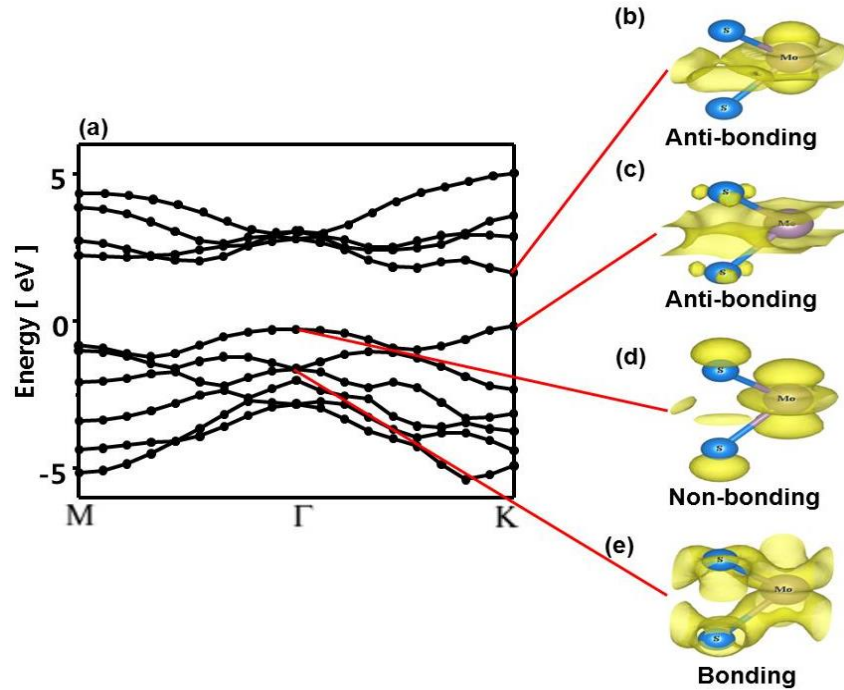


Fig. 2 The electronic band structure of the MoS<sub>2</sub> monolayer and the wave functions at some points (a) The electronic band structure of monolayer MoS<sub>2</sub>, (b) the CBM at the K point, (c) the VBM at the K point, (d) the VBM at the  $\Gamma$  point, and (e) the second highest valence band at the  $\Gamma$  point

atoms (e), respectively. Note that the VBM at the  $\Gamma$  point is the non-bonding state, which is rarely affected by the deformation of crystal structure under mechanical strain. Meanwhile, the VBM and the CBM at the K point have anti-bonding characters, indicating that a relatively larger energy shift at the K point is possible due to the change of the wave function overlap by crystal structure deformation.

In order to investigate the effect of mechanical strains on the electronic characteristics of the MoS<sub>2</sub> monolayer, we applied mechanical strains to the MoS<sub>2</sub> monolayer with (i) uniaxial strain in the  $x$  or  $y$  directions, (ii) biaxial strain in the  $x$  and  $y$  directions, and (iii) pure shear strain by changing the angle between the  $a$  and  $b$  vectors shown in Fig. 1(a). The changes of the band-gap energy of the MoS<sub>2</sub> monolayer due to the corresponding mechanical strains are summarized in Fig. 3. Open and solid circles denote the direct and indirect band-gap types, respectively. The band gap energy is drastically changed under biaxial strain, but it is changed a little under pure shear strain, as shown in Figs. 3(a) and (b), respectively. In other words, the strain range for the direct band-gap is much smaller under biaxial strain than under pure shear strain. The band gap changes due to uniaxial strains in the  $x$  and  $y$  directions show similar results, although uniaxial strain in the  $y$  direction makes a slightly larger change than that in the  $x$  direction. All variations in the band gap energy are highly asymmetric. The band-gap energy shows a larger reduction under all types of tensile strains, but it increases to strains of 1-3% and decreases as compressive strains increase. Interestingly, we found that the band-gap energies at the transition points from a direct to an indirect band-gap are almost the same under all types of strain modes, although the corresponding strains at the transition points differ depending on the strain mode. The band-gap energies at the

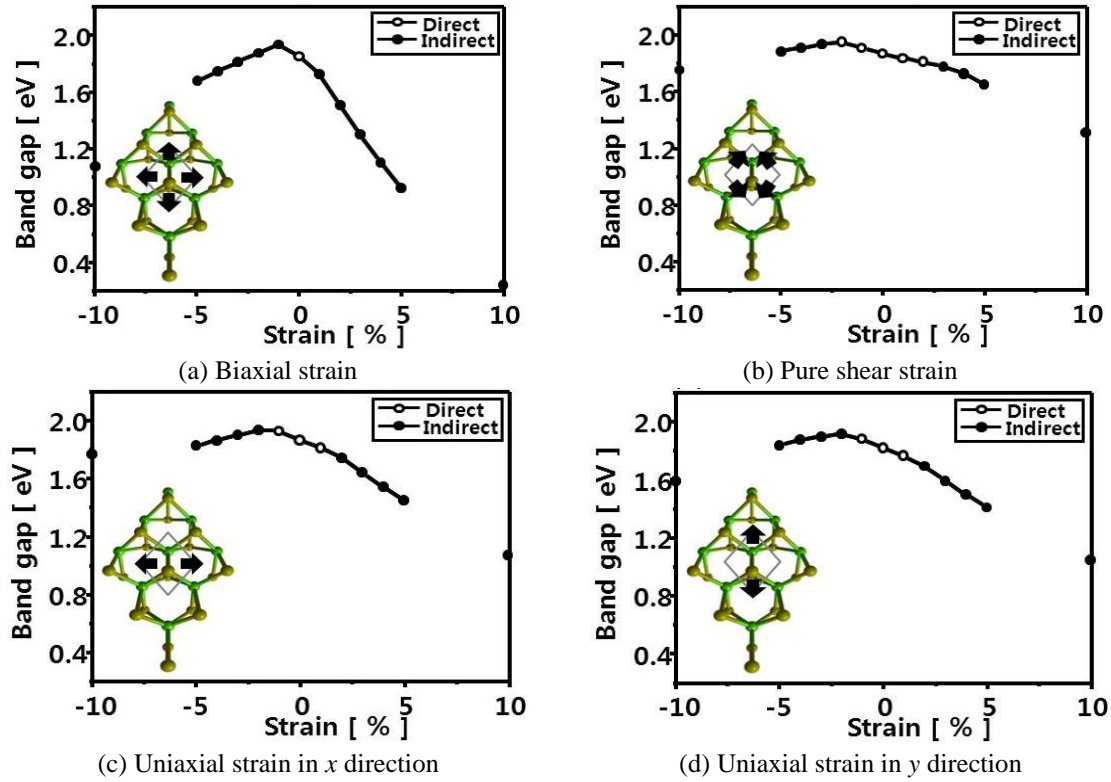


Fig. 3 The variation in the band-gap energies for different mechanical strains

transition points under all types of strain modes are found to be about 1.74 eV in tension and 1.91 eV in compression, respectively. It should also be noted that the transitions occur near or at the maximum values of the band-gap energy, when compressive strains are applied, as shown in Fig. 4.

When biaxial strain is applied, the strains for the transition from a direct to an indirect band-gap are found to be about 0.7% in tension and 0.7% in compression. Here, the bond lengths between Mo and its neighboring S atoms increase by 0.005 Å (~0.21%) in tension and decrease by 0.003 Å (~0.13%) in compression compared to the unstrained MoS<sub>2</sub> monolayer. The changes in the bond angles between Mo and its neighboring two S atoms in a hexagonal ring are found to be 0.50° in tension, and -0.58° in compression. Under the pure shear strain, the transition strains are found to be about 2.6% in tension and 2.0% in compression. In cases of uniaxial strains, the transition initiates at smaller strain in the  $x$  direction (~1.3%) than in the  $y$  direction (~1.6%) under compression, while the transition strains are the same (~1.5%) in both directions under tension. Because uniaxial strains break the symmetry of the crystal structure, we found that the changes in bond lengths and angles differ depending on the bond considered and the direction of deformation. For example, the bonds along the  $y$  direction are stretched by up to 0.008 Å (~0.34%), while the changes in other bonds are less than 0.002 Å at the transition point under uniaxial tensile strain in the  $y$  direction. We summarize the critical strains (lower values) for the maximum band-gap and the direct-indirect transition and the corresponding band-gap energies (upper values) under different deformation modes in Table 2.

Table 2 The maximum energy band-gap and two transition points under different strain types: The lower values are the critical strains (%) at the maximum and transitions, and the upper values area band-gap energies (eV) under the strains

Strain types	Maximum gap	Transition (Compression)	Transition (Tension)
Biaxial	1.92	1.92	1.73
	-0.80	-0.07 ~ -0.08	0.07 ~ 0.08
Pure shear	1.91	1.91	1.73
	-2.00	-2.00 ~ -2.10	2.60 ~ 1.60
Uniaxial (X)	1.92	1.91	1.73
	-1.40	-1.30 ~ -1.40	1.50 ~ 1.60
Uniaxial (Y)	1.94	1.93	1.73
	-1.70	-1.60 ~ -1.70	1.50 ~ 1.60

The dependence of the band-gap changes upon the mechanical strain directions can be explained with the crystal structures shown in Fig. 3. A single Mo atom in MoS<sub>2</sub>, has six bonds with six neighboring S atoms. Since biaxial strain deformation changes all the distances between the Mo atom and its six neighboring S atoms, the change of the electrons' interaction between the Mo atom and the S atoms is the largest, and the corresponding energy shift is the largest as well, as long as the same amount of strain is applied. On the other hand, because pure shear strain mainly alters the bond angles between the Mo atom and the S atoms with a negligible distance variation, the band gap change is minimal among the considered deformations, within the small strain range we considered. In other words, we need to apply a relatively large amount of strain, in order to induce a sufficient band-gap change by using pure shear deformation. Uniaxial strain in the *x* or *y* direction affects the distance between the Mo atom and the six S atoms like biaxial strain, but the degree of the distance change is smaller, and thus the band-gap change is smaller compared to the biaxial case, under the same amount of strain. Due to the largest changes in the crystal structure, the strain range of the direct band-gap is the narrowest when a biaxial strain is applied, as shown in Figs. 3(a) and 4(a). Even at a biaxial strain of 0.7% (either compressive or tensile), the band-gap of the MoS<sub>2</sub> monolayer becomes indirect.

In the sense of the band-gap type, pure shear strain is the most stable deformation to keep the band-gap direct. Up to a compressive pure shear strain of 2%, the band-gap of the MoS<sub>2</sub> monolayer remains direct. In order to keep the band-gap of the MoS<sub>2</sub> monolayer direct for optoelectronic device applications, one should not allow the strains to exceed their critical values. The band-gap, which is found to be direct at the K point under small strain, changes to indirect as strain increases.

As the tensile strain increases further, the energy of the VBM at the K point becomes lower than that at the  $\Gamma$  point, while the lowest value of the CBM remains at the K point. As a result, the indirect gap consists of the VBM at the  $\Gamma$  point and the CBM at the K point, under all types of tensile strain. However, when the compressive strain increases, while the highest energy point of the VBM remains at the K point, the energy of the CBM at the middle of  $\Gamma$ -K points becomes the lowest. Thus, the indirect gap consists of the VBM at the K point and the CBM at the middle of  $\Gamma$ -K points under all types of compressive deformations. These results are consistent with the previous report (Yun and Han 2012), which showed the same indirect pathway for biaxial strain.

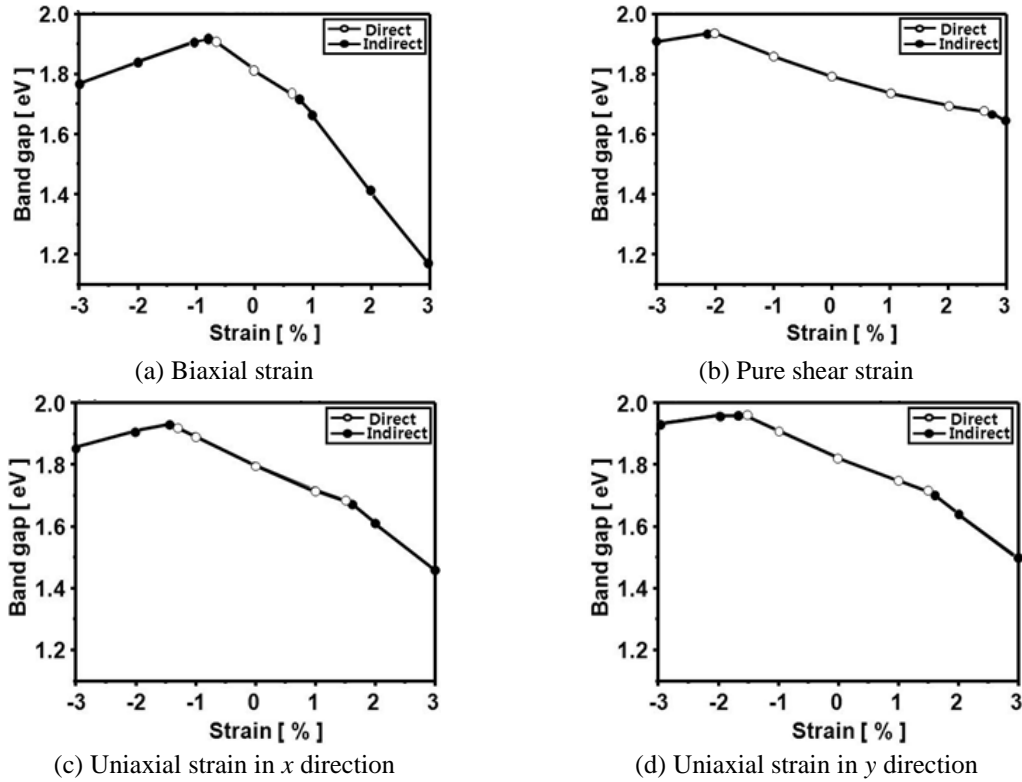


Fig. 4 The variation in band-gap energy under different strains

The band-gap transition from direct to indirect and the variations of the band gap energy can be explained by the change of the electronic structures caused by mechanical strains. To accomplish this, we plot the variation in the electronic band structure with different strains in Figs. 5(a) to (d). Only the VBMs (solid lines) and the CBMs (dashed lines) from the  $\Gamma$  point to the K point are shown for clarity. To visualize the change of the electronic structure, we plot the electronic wave functions of the VBM at the  $\Gamma$  and K points under different amounts of biaxial strain, as shown in Figs. 5(e) and (f), respectively. In all the considered cases, the energy shifts of the VBM at the  $\Gamma$  point in response to mechanical strains are relatively small, because the VBM at the  $\Gamma$  point shows a non-bonding character as discussed in Fig. 2. However, the energy shifts of the VBM at the K point based on the strains are large enough to initiate the changes of the band-gap type. As the compressive strain increases, the CBM (red and blue dotted lines) and the VBM (red and blue solid lines) at the K point increase under all types of strain modes. It should be noted that since the VBM and the CBM at the K point have anti-bonding characters, their energies increase as the overlap of wave functions increases. Therefore, because negative strains make the overlap increase, the VBM and the CBM at the K point under compressive strain are higher than those of the unstrained bands (black line) in all the cases considered. Consistently, the VBM and the CBM at the K point (sky blue and pink lines) are lower than those of the unstrained bands under tensile strain, because positive strains decrease the overlap of wave functions. These changes in the overlap of wave functions at the K point due to mechanical strain are clearly shown in Fig. 5(f), compared to small changes at the  $\Gamma$  point in Fig. 5(e).

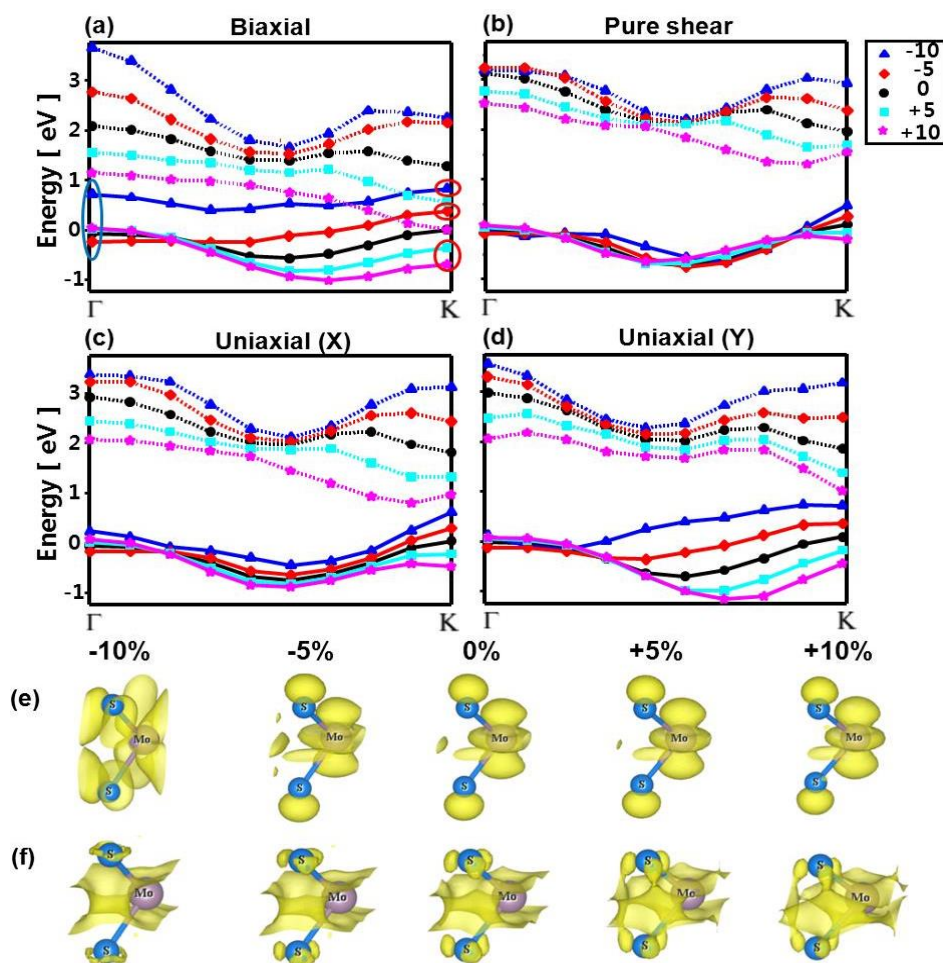


Fig. 5 The variation in the electronic band structure and the wave functions of the MoS<sub>2</sub> monolayer for different strains: The variation in the band structure under (a) biaxial strain, (b) pure shear strain, (c) uniaxial strain in the  $x$  direction, (d) uniaxial strain in the  $y$  direction, and the variation in the wave functions of the VBM (e) at the  $\Gamma$  point and (f) at the K point. The numbers above (e) and (f) are the amounts of biaxial strain

#### 4. Conclusions

We have performed first-principles calculations to investigate the effect of mechanical strains on the electronic properties of a single layer of MoS<sub>2</sub>. For this, we applied uniaxial, biaxial and pure shear strains, and discussed the change in the band-gap energy based on the applied strains. We found that the band-gap energy changes more under biaxial strain, because it induces a larger deformation in the crystal structure of the MoS<sub>2</sub> monolayer resulting in a larger change in the overlapping of the wave functions. We also found that the band structure of the MoS<sub>2</sub> monolayer changes from direct to indirect for all types of strains, and we obtained the critical strains of the transition for different strain types. All calculations show that mechanical strain is an effective way to control and tune the electronic properties of MoS<sub>2</sub>.

## Acknowledgments

This work was done with financial support from the Mid-Career Researcher Support Programs and through the National Research Foundation (NRF) of Korea funded by the Ministry of Education, Science, and Technology (MEST) (Grant No. 2014R1A2A09052374). We gratefully acknowledge the supercomputing resources of the PLSI of the Korea Institute of Science and Technology Information (KISTI) and the UNIST Supercomputing Center.

## References

- Ataca, C. and Ciraci, S. (2011), "Functionalization of single-layer MoS<sub>2</sub> honeycomb structures", *J. Phys. Chem. C*, **115**(27), 13303-13311.
- Bloch, P.E. (1994), "Projector augmented-wave method", *Phys. Rev. B*, **50**(24), 17953.
- Dan, Y.P., Lu, Y. and Kybert, N.J. (2009), "Intrinsic response of graphene vapor sensors", *Nano Lett.*, **9**(4), 1472-1475.
- Joensen, P. and Crozier, E.D. (1987), "A study of single-layer and restacked MoS<sub>2</sub> by x-ray diffraction and x-ray absorption spectroscopy", *J. Phys. C: Sol. State Phys.*, **20**(26), 4043-4053.
- Kam, K.K. and Parkinson, B. (1982), "Detailed photocurrent spectroscopy of the semiconducting group VIB transition metal dichalcogenides", *J. Phys. Chem.*, **86**(4), 463-467.
- Kim, S.Y. and Park, H.S. (2010), "On the utility of vacancies and tensile strain-induced quality factor enhancement for mass sensing using graphene monolayers", *Nanotech.*, **21**(10), 105710.
- Kress, G. and Furthmuller, J. (1996a), "Efficiency of ab-initio total energy calculations for metals and semiconductors using a plane-wave basis set", *Mater. Sci.*, **6**(1), 15-50.
- Kress, G. and Furthmuller, J. (1996b), "Efficient iterative schemes for ab initio total-energy calculations using a plane-wave basis set", *Phys. Rev. B*, **54**(16), 11169.
- Kress, G. and Hafner, J. (1993), "Ab initio molecular dynamics for open-shell transition metals", *Phys. Rev. B*, **48**(17), 13115.
- Lee, C., Wei, X.D. and Kysar, J.W. (2008), "Measurement of the elastic properties and intrinsic strength of monolayer graphene", *Sci.*, **321**(5887), 385-388.
- Mak, K.F., Lee, C. and Hone, J. (2010), "Atomically thin MoS<sub>2</sub>: A new direct-gap semiconductor", *Phys. Rev. Lett.*, **105**(13), 136805.
- Monkhorst, H.J. and Pack, J.D. (1976), "Special points for brillouin-zone integrations", *Phys. Rev. B*, **13**(12), 5188.
- Novoselov, K.S. (2004), "Electric field effect in atomically thin carbon films", *Sci.*, **306**(5696), 666-669.
- Novoselov, K.S. and Geim, A.K. (2005), "Two-dimensional gas of massless dirac fermions in graphene", *Nat.*, **438**(7065), 197-200.
- Obradovic, B., Kotlyar, R. and Heinz, F. (2006), "Analysis of graphene nanoribbons as a channel material for field-effect transistors", *Appl. Phys. Lett.*, **88**(14), 142102.
- Perder, J.P. and Chevary, J.A. (1992), "Atoms, molecules, solids, and surfaces: Applications of the generalized gradient approximation for exchange and correlation", *Phys. Rev. B*, **46**(11), 6671.
- Perdew, J.P. and Zunger, A. (1981), "Self-interaction correction to density-functional approximations for many-electron systems", *Phys. Rev. B*, **23**(10), 5048.
- Radisavljevic, B., Radenovic, A. and Giacometti, V. (2011), "Single-layer MoS<sub>2</sub> transistor", *Nat. Nanotech.*, **6**(3), 147-150.
- Vanderbit, D. (1990), "Soft self-consistent pseudopotentials in a generalized eigenvalue formalism", *Phys. Rev. B*, **41**(11), 7892.
- Yun, W.S., Han, S.W. and Hong, S.C. (2012), "Thickness and strain effects on electronic structures of transition metal dichalcogenides: 2H-MX<sub>2</sub> semiconductors (M=Mo, W; X=S, Se, Te)", *Phys. Rev. B*,

**85**(3), 033305.

Zhang, Y.B., Tan, Y.W. and Stromer, H.L. (2005), "Experimental observation of the quantum hall effect and berry's phase in graphene", *Nat.*, **438**(7065), 201-204.

*MC*